Intestinal de novo phosphatidylcholine synthesis is required for dietary lipid absorption and metabolic homeostasis[S]

John P. Kennelly,*,† Jelske N. van der Veen,*,§ Randal C. Nelson,* Kelly-Ann Leonard,*,† Rick Havinga,,†† Jean Buteau,† Folkert Kuipers,**,†† and René L. Jacobs[1,*,†,§]**

Group on the Molecular and Cell Biology of Lipids* and Departments of Agricultural, Food and Nutritional Science† and Biochemistry,§ University of Alberta, Edmonton, Alberta, Canada; and Departments of Pediatrics** and Laboratory Medicine,†† University of Groningen, University Medical Center Groningen, Groningen, The Netherlands

ORCID IDs: 0000-0002-4399-3976 (J.P.K); 0000-0002-5525-1355 (R.L.J.)

Abstract De novo phosphatidylcholine (PC) synthesis via CTP:phosphocholine cytidylyltransferase-α (CTα) is required for VLDL secretion. To determine the precise role of de novo PC synthesis in intestinal lipid metabolism, we deleted CTα exclusively in the intestinal epithelium of mice (CTα^{IKO} mice). When fed a chow diet, CTα^{IKO} mice showed normal fat absorption despite a ~30% decrease in intestinal PC concentrations relative to control mice, suggesting that biliary PC can fully support chylomicron secretion under these conditions. However, when fed a high-fat diet, CTα^{IKO} mice showed impaired passage of FAs and cholesterol from the intestinal lumen into enterocytes. Impaired intestinal lipid uptake in CTα^{IKO} mice was associated with lower plasma triglyceride concentrations, higher plasma glucagon-like peptide 1 and peptide YY, and disruption of intestinal membrane lipid transporters after a high-fat meal relative to control mice. Unexpectedly, biliary bile acid and PC secretion was enhanced in CTα^{IKO} mice due to a shift in expression of bile-acid transporters to the proximal intestine, indicative of accelerated enterohepatic cycling. These data show that intestinal de novo PC synthesis is required for dietary lipid absorption during high-fat feeding and that the reacylation of biliary lyso-PC cannot compensate for loss of CTα under these conditions.—Kennelly, J. P., J. N. van der Veen, R. C. Nelson, K-A. Leonard, R. Havinga, J. Buteau, F. Kuipers, and R. L. Jacobs. **Intestinal de novo phosphatidylcholine synthesis is required for dietary lipid absorption and metabolic homeostasis. *J. Lipid Res*. 2018.** 59: **1695–1708.**

Supplementary key words bile • phospholipids • lipids and lipoprotein metabolism • chylomicrons • triglycerides • intestine • glucagon-like peptide 1 • peptide YY

Phospholipids form the matrix of biological membranes, provide precursors for a variety of signaling molecules, and allow assembly and secretion of lipoproteins (1). Phosphatidylcholine (PC) is the primary phospholipid in eukaryotic cells (1). The amphitropic enzyme CTP:phosphocholine cytidylyltransferase (CT) regulates de novo PC synthesis in response to changes in membrane lipid composition in all nucleated mammalian cells (2). Global deletion of CTα (encoded by *Pcyt1a*) is embryonic lethal in mice, reflecting the essential role of membrane biogenesis during development (3). Mice lacking CTα in the liver have impaired VLDL secretion and accumulate neutral lipids in hepatocytes (4), despite the presence of a second route for hepatic PC synthesis via the methylation of phosphatidylethanolamine (PE) by phosphatidylethanolamine-*N*-methyltransferase (PEMT). Similarly, CTα cannot compensate for the loss of PEMT in generating PC for VLDL assembly (5).

Intestinal PC can be derived from the diet, bile, circulating lipoproteins, and local de novo synthesis. Dietary and biliary PC is hydrolyzed in the intestinal lumen by phospholipase A2 to lyso-PC and FAs before being absorbed into enterocytes, delivered to the endoplasmic reticulum, and reacylated into PC by lyso-PC acyltransferase enzymes (6, 7). Mice lacking hepatic *Abcb4*, which is required for PC secretion into bile, have normal passage of

This work was supported by Canadian Institutes of Health Research Grant 156243 (to R.L.J), the Alberta Diabetes Institute (to R.L.J and J.P.K), and Alberta Innovates–Technology Futures (to J.P.K).

Manuscript received 16 May 2018 and in revised form 6 July 2018.

Published, JLR Papers in Press, July 14, 2018
DOI https://doi.org/10.1194/jlr.M087056

Abbreviations: *Cd36*, *Cluster-determinant 36*; CT, CTP:phosphocholine cytidylyltransferase; *Fabp6*, Fatty acid binding protein 6; FGF21, fibroblast-like growth factor 21; FPLC, fast protein liquid chromatography; GLP-1, glucagon-like peptide 1; HFD, high-fat diet; *Mogat2*, *monoacylglycerol O-acyltransferase 2*; *Npc1l1*, *NPC1 like intracellular cholesterol transporter 1*; PC, phosphatidylcholine; PE, phosphatidylethanolamine; PYY, peptide YY; *Slc10a2*, *solute carrier family 10 member 2*; *Slc27a4*, *Solute Carrier Family 27 Member 4*; TG, triglyceride.

[1] To whom correspondence should be addressed.
email: rjacobs@ualberta.ca

[S] The online version of this article (available at http://www.jlr.org) contains a supplement.

FAs from the intestinal lumen into enterocytes but have impaired chylomicron assembly and secretion, highlighting the importance of biliary PC for chylomicron output (8). Furthermore, loss of intestinal lysophosphatidylcholine acyltransferase 3 (*Lpcat3*), which incorporates PUFAs into PC, impairs dietary lipid absorption despite maintenance of total intestinal PC mass (9, 10). Conversely, increasing the delivery of PC to the intestinal lumen promotes chylomicron secretion (11). Therefore, although the reacylation of lyso-PC derived from the intestinal lumen is important for chylomicron production, the precise contribution that intestinal de novo PC synthesis makes to this process is unknown.

In the present study, we hypothesized that loss of intestinal CTα activity would cause triglyceride (TG) accumulation in enterocytes due to insufficient supply of PC for chylomicron assembly. However, we unexpectedly found that loss of intestinal de novo PC synthesis impairs passage of FAs from the intestinal lumen into enterocytes in the setting of a high-fat diet (HFD), but not a chow diet. Fat malabsorption is linked to the repression of genes involved in FA uptake, enhanced postprandial enteroendocrine hormone secretion, and reduced adiposity. Furthermore, we show that loss of intestinal CTα promotes biliary bile acid and lipid secretion by accelerating enterohepatic bile acid cycling. Our data provide evidence of a specific requirement for intestinal de novo PC synthesis in the maintenance of intestinal metabolic functions and show that the reacylation of lyso-PC from extraintestinal sources is insufficient to maintain metabolic function during HFD feeding.

MATERIALS AND METHODS

Generation of mice with intestine-specific deletion of *Pcyt1a*

Mice carrying a floxed *Pcyt1a* locus ($Pcyt1a^{LoxP/LoxP}$) on a C57BL/6J background were crossed with mice expressing a tamoxifen-inducible Cre-recombinase transgene under the control of a villin promoter (villin-$CreER^{T2}$) (12) to generate $Pcyt1a^{LoxP/WT}$;villin-$CreER^{T2}$ mice (with the capacity to induce a heterozygous deletion of intestinal CTα after tamoxifen treatment). Subsequent cross-breeding of $Pcyt1a^{LoxP/WT}$;villin-$CreER^{T2}$ mice resulted in the generation of $Pcyt1a^{LoxP/LoxP}$;villin-$CreER^{T2}$ mice (with the capacity to induce a homozygous deletion of intestinal CTα after tamoxifen treatment). Genomic DNA was extracted from tail biopsies with a DNeasy Blood and Tissue Kit (Qiagen, UK). PCR products were identified on a 3% agarose gel (floxed *Pcyt1a* band) or a 1.5% agarose gel (Villin Cre-inducible band). Cre was induced in 8–12 week old male or female mice by intraperitoneal injection of tamoxifen (1 mg/day in sunflower oil for 5 days; Sigma, St. Louis, MO), while tamoxifen-treated $Pcyt1a^{LoxP/LoxP}$ mice were used as controls. Mice were fed a chow diet (5001, Lab Diet, St. Louis, MO) or a semipurified HFD containing 40% kilocalories as fat (supplemental Table S1). Mice were housed in a temperature-controlled room with 12 h light/dark cycle and free access to food and water. Samples were collected after a 10 h fast or after overnight fasting followed by 2 h refeeding, unless otherwise stated. Small intestines were excised, flushed with PBS containing protease inhibitor cocktail (Sigma), and kept on ice. The small intestine was divided into three portions of length ratio 1:3:2 (corresponding to duodenum:jejunum:ileum) before jejunum sections were fixed in 10% neutral-buffered formalin for histology. Epithelial cells were collected in liquid nitrogen after segments were opened longitudinally. The University of Alberta's Institutional Animal Care Committee approved all animal procedures, which were in accordance with guidelines of the Canadian Council on Animal Care.

Microscopy

Formalin-fixed, paraffin-embedded tissue slices (5 μm thick) were stained with H&E and visualized with a light microscope. For electron microscopy, 2 cm jejunal rings were fixed with 2% paraformaldehyde and 2.5% glutaraldehyde in 0.1 M phosphate buffer (pH 7.2). Sections were cryosectioned with an ultramicrotome (Ultracut E, Reichert-Jung) equipped with an FC4D attachment, and images were obtained using a Philips 410 transmission electron microscope.

mRNA isolation and quantification by PCR

Total RNA was isolated from intestinal scrapings or liver using Trizol (Invitrogen, CA). RNA was reversed-transcribed using Superscript II (Invitrogen). Quantitative PCR was run on an Applied Biosystems StepOne Plus for 40 cycles using a Power SYBR Green PCR Master Mix (Applied Biosystems, MA), in triplicate. Relative mRNA expression was normalized to cyclophilin. Quantitation was performed using the standard curves method. Primer sequences are listed in supplemental Table S2.

FA absorption

Intestinal FA absorption was quantified as described previously (13), with modifications. Briefly, male control and $CT\alpha^{IKO}$ mice were fasted for 4 h before receiving an oral gavage of 150 μl of olive oil containing 5 μCi [^{3}H]-labeled triolein. Blood was collected at 30, 60, 90, and 120 min postgavage. At 120 min postgavage, the small intestine was excised, flushed with 40 ml of PBS containing 0.5 mM sodium taurocholate, and cut into 2 cm segments. Segments were dissolved in 1 N NaOH for 3 days at 60°C. Plasma and tissue [^{3}H]-label was measured by liquid scintillation counting (Beckman Coulter Inc., CA). For poloxamer studies, mice were fasted for 10 h before receiving an intraperitoneal injection of Poloxamer-407 (1 g/kg; Sigma) and an oral gavage of 150 μl olive oil. Blood was collected before and every hour for 4 h after the oil challenge. Plasma TG concentrations were assessed using a commercially available kit (Sekisui Diagnostics, MA). To visualize intestinal lipid droplets after a fat challenge, 4 h fasted female mice were gavaged (7.5 μl/g mouse) with olive oil containing 20% BODIPY 500/510 C1, C12 (catalog no. D3823, Invitrogen). Sections of the proximal small intestine were embedded in OCT and sliced on a cryostat at −20°C. Slides were mounted with Prolong Diamond Antifade Mountant containing DAPI (catalog no. P36962, Invitrogen) before images were obtained with a fluorescence microscope (Olympus, Markham, ON) equipped with Suveyor and Image-Pro Plus software.

Cholesterol absorption

Individually housed male control and $CT\alpha^{IKO}$ mice received an oral dose of [^{3}H]cholesterol (2 μCi) with 6 mg of unlabeled cholesterol in 150 μl of olive oil and an intravenous injection of [^{14}C]cholesterol (1 μCi) mixed in Intralipid®. Blood and feces was collected at 24, 48, and 72 h after cholesterol administration. Blood was centrifuged at 3,000 *g* for 10 min, and plasma was collected. Plasma [^{3}H]- and [^{14}C]-label was measured by liquid scintillation counting (Beckman Coulter Inc.). The [^{3}H]- and [^{14}C]-label in fecal neutral sterol and fecal bile salt (aqueous)

fractions were measured by liquid scintillation counting (Beckman Coulter Inc.) after separation of the fractions by the method of Folch et al. (14).

Gallbladder cannulations and bile measurements

For gallbladder cannulations, male mice were anesthetized by intraperitoneal injection of ketamine (100 mg/kg)/ xylazine (10 mg/kg). Gallbladders were cannulated with silastic tubing (Dow Corning, MI; internal diameter 0.5 mm) after ligation of the common bile duct beside the duodenum. Mice were placed in a humidified incubator, and bile was collected for 30 min in preweighed vials. Bile acid species composition [including tauro-hyodeoxycholic acid, tauro-β-muricholic acid, tauro-α-muricholic acid, β-muricholic acid, taurodeoxycholic acid (TDCA), tauro-chenodeoxycholic acid, taurocholic acid, tauroursodeoxycholic acid, and cholic acid] was determined by LC/MS/MS as described previously (15). The hydrophobicity of bile acids was determined according to the method of Heuman (16). Biliary lipids were extracted by the method of Folch et al. (14). Biliary phospholipid concentrations were assessed by phosphorous assay, as described previously (17). Biliary cholesterol concentrations were measured with a commercially available kit (WAKO Chemicals). Biliary secretion rates were calculated by multiplying biliary bile acid, phospholipid, or cholesterol concentrations by bile flow (μl/min). Bile acid concentrations in feces and plasma were determined by enzymatic fluorometric assay (18).

Plasma, tissue, and fecal lipid analysis

Plasma TG (Sekisui Diagnostics), cholesterol (Wako Chemicals), and NEFAs (Wako Chemicals) were measured with commercially available kits. Lipoprotein fractions were separated from pooled plasma samples (five mice per group) by size exclusion fast protein liquid chromatography (FPLC) before measuring TG and cholesterol concentrations by commercially available kits (Lipidomics Core Facility, University of Alberta). Total protein concentrations of tissue homogenates were determined by bicinchoninic acid assay before tissue lipids were extracted from homogenates (1 mg/ml) by the method of Folch et al. (14). PC and phosphatidylethanolamine (PE) were separated by thin layer chromatography using the solvent system chloroform:methanol:acetic acid:water (50:30:8:4). Bands were visualized after exposure to iodine and measured by phosphorous assay, as described previously (17). Intestinal TG concentrations were measured using a commercially available kit (Sekisui Diagnostics). The relative abundance of PC species in jejunal epithelial cells was measured by mass spectrometry at The Metabolomics Innovation Centre, University of Alberta. To analyze the FA composition of intestinal PC, lipids were extracted from intestinal scrapings and separated by TLC as described above. PC bands were recovered from the plates and converted to FA methyl esters by incubation with 2 ml of hexane (Sigma-Aldrich, 293253) and 1.5 ml of boron trifluoride (Sigma-Aldrich, B1252) in methanol for 1 h at 110°C. FA methyl esters were then analyzed by gas-liquid chromatography (results are shown as the percentage of total FAs measured). Intestinal nonesterified cholesterol and cholesterol esters were measured by gas-liquid chromatography with flame ionization detection after derivatization with bis(trimethylsilyl) trifluoroacetamide and adjustment of peaks with the internal standard tridecanoin, as described previously (19). Fecal samples (50 mg) were dried and ground to a powder before extraction of lipids by the method of Folch et al. (14). NEFA and cholesterol concentrations in feces of female mice collected over 72 h were determined with commercially available kits (Wako Chemicals).

Measurement of intestinal CT activity

Intestinal CTα activity was determined by measuring the conversion of [^{3}H]phosphocholine into [^{3}H]CDP-choline, as described previously (4).

Plasma metabolite measurements

Blood glucose was measured from the tail vein with a glucometer (Accu-chek, Roche, Switzerland) after a 10 h fast, after 2 h refeeding, or after 2 h refeeding followed by an oral gavage of glucose (2 mg/g body weight). Blood was collected by cardiac puncture in tubes containing EDTA, dipeptidyl peptidase 4 inhibitor (EMD Millipore, MA), and Complete® general protease inhibitor (Sigma) before being centrifuged at 3,000 *g* for 10 min to obtain plasma. Plasma insulin (Meso Scale Diagnostics, MD), leptin (Meso Scale Diagnostics), active glucagon-like peptide 1 (GLP-1) (EMD Millipore), peptide YY (PYY) (Crystal Chem, IL), and fibroblast-like growth factor 21 (FGF21) (Abcam, Cambridge, UK) were measured by ELISA, according to the manufacturer's instructions. Plasma (4 μl) was resolved on a sodium dodecyl sulfate polyacrylamide gel (5% gel for ApoB and 10% for ApoA1). Proteins were transferred to a to a PVDF membrane and probed with either anti-ApoB (dilution 1:7,500; catalog no. AB742, Chemicon, MA) or anti-ApoA1 (dilution 1:2,000; catalog no. K23001R, BioDesign/Meridian). ApoB and ApoA1 were run on separate gels. Immunoreactive proteins were detected with ECL (Amersham, GE Healthcare, UK), and blots were imaged with a Chemi-Doc MP Imager, (Bio-Rad Laboratories, CA).

Statistics

Data are expressed as mean ± SEM using GraphPad Prism 7 (GraphPad Software, La Jolla, CA); $P < 0.05$ was considered statistically significant. Student's *t*-test was used to compare two independent groups. A one-way ANOVA was used when comparing three groups with one experimental outcome. A two-way ANOVA with Bonferroni posttest was used to determine the effect of genotype and time on an experimental outcome.

RESULTS

Intestinal PC concentrations are reduced in CTα^{IKO} mice fed a chow diet, but fat absorption capacity is unaltered

Induction of Cre recombinase with tamoxifen in *Pcyt1a*$^{LoxP/LoxP}$;villin-CreER^{T2} mice (herein referred to as CTα^{IKO} mice) reduced *Pcyt1a* mRNA abundance and CTα enzyme activity in the jejunum and ileum by >90% compared with tamoxifen-treated *Pcyt1a*$^{LoxP/LoxP}$ control mice (**Fig. 1A**, B and supplemental Fig. S1A). *Pcyt1a* mRNA remained repressed in the intestines of CTα^{IKO} mice for at least 50 days following Cre induction (supplemental Fig. S1B). Characterization of mice with a heterozygous deletion of intestinal CTα fed either a chow diet (supplemental Fig. S1D–H) or a HFD (supplemental Fig. S1I–M) revealed no differences in body weight, blood glucose, plasma lipids, or fat absorption after an oral lipid bolus, despite a ∼50% decrease in intestinal *Pcyt1a* mRNA abundance compared with control mice (supplemental Fig. S1C).

Loss of intestinal CTα did not impact survival of the mice fed the chow diet, and body mass of CTα^{IKO} mice was comparable to that of controls after 6 weeks (Fig. 1C). Furthermore, histological examination of H&E-stained jejunum sections at 6 weeks after Cre induction revealed no overt

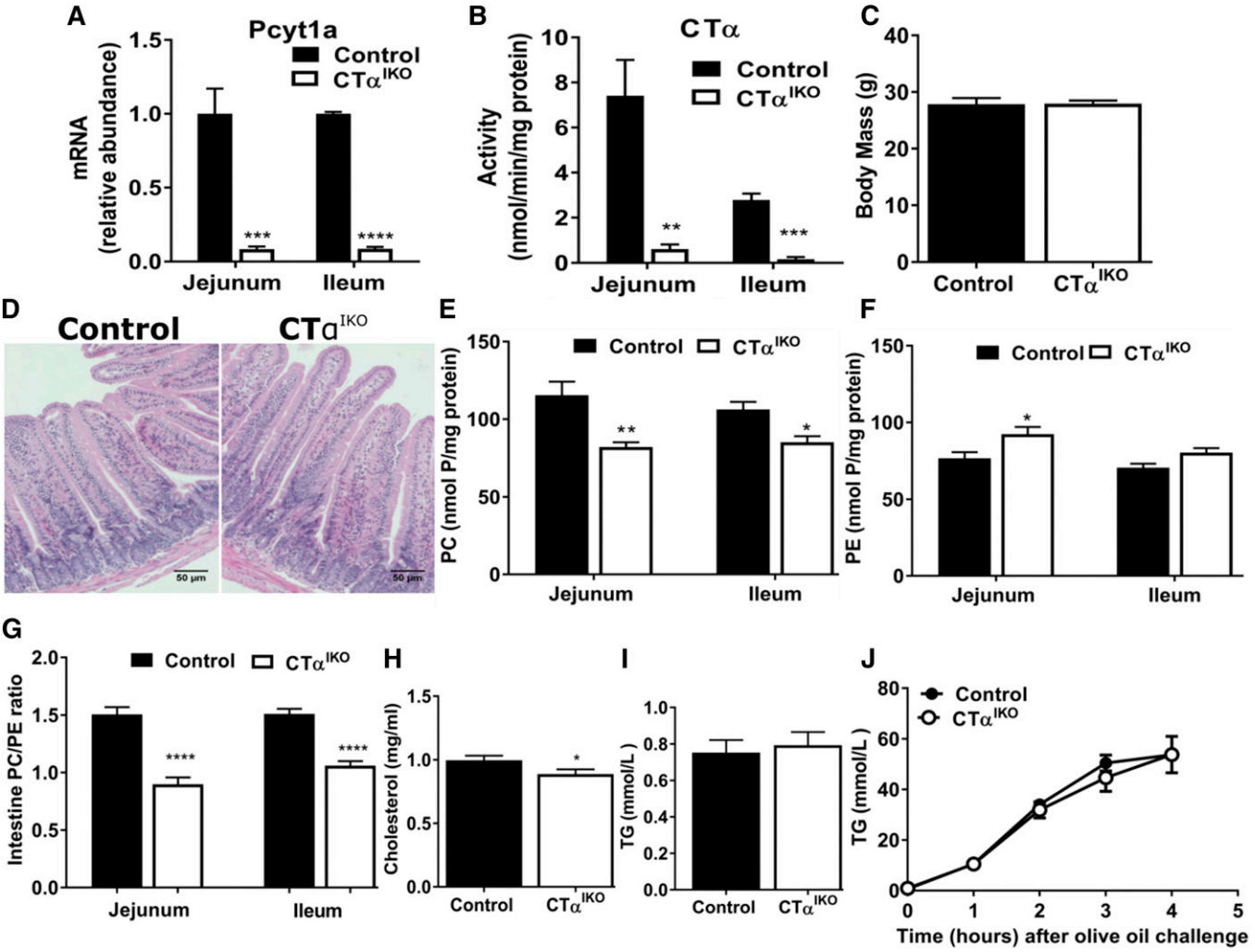

Fig. 1. Intestinal PC concentrations are reduced in CTα^{IKO} mice fed a chow diet, but fat absorption capacity is unaltered. *Pcyt1a* mRNA abundance (A) and CTα enzyme activity (B) in the jejunum and ileum of control and CTα^{IKO} mice 5 days after Cre induction. Male control and CTα^{IKO} mice were fed a chow diet for 6 weeks following Cre induction before being fasted for 10 h, intraperitoneally injected with Poloxamer-407, and gavaged with olive oil. C: Fasting body mass of male control and CTα^{IKO} mice fed the chow diet for 6 weeks (n = 10 or 11 per group). D: Representative H&E-stained jejunum sections from control and CTα^{IKO} mice fed the chow diet for 6 weeks. E: PC concentrations in the jejunum and ileum (n = 5 per group). F: PE concentrations in the jejunum and ileum (n = 5 per group). G: Molar ratio of PC-to-PE in the jejunum and ileum (n = 5 per group). Fasting plasma cholesterol (H), fasting plasma TG (I), and plasma TG (J) before and 1, 2, 3, and 4 h following the oral bolus of olive oil in mice fed the chow diet for 6 weeks. Values are means ± SEM, n = 5 per group. * $P < 0.05$; ** $P < 0.01$; *** $P < 0.001$; **** $P < 0.0001$.

morphological abnormalities in CTα^{IKO} intestines compared with control intestines (Fig. 1D). This finding suggests that intestinal CTα activity is not required for maintenance of epithelial cell turnover in adult mice. PC concentrations were lower in the jejunum and ileum of CTα^{IKO} mice compared with controls after an oil challenge (Fig. 1E). Furthermore, PE concentrations were higher in the jejunum of CTα^{IKO} mice (Fig. 1F). This resulted in a relatively large decrease in the molar ratio of PC-to-PE in the intestines of CTα^{IKO} mice (Fig. 1G). Fasting plasma cholesterol concentrations (Fig. 1H) were significantly lower in CTα^{IKO} mice fed the chow diet, whereas fasting plasma TG (Fig. 1I), insulin, and blood glucose concentrations (not shown) were unchanged compared with control mice.

Unexpectedly, despite the absence of intestinal CTα activity and a dramatic decrease in the PC/PE ratio of intestinal membranes, TG appearance in plasma was comparable between CTα^{IKO} mice and control mice after an oral bolus of olive oil (Fig. 1J). This finding suggests that, in contrast to the liver where "new" PC synthesis is required for VLDL secretion (4), intestinal de novo PC synthesis is dispensable for chylomicron secretion in the setting of a low-fat diet. These results also suggest that PC supplied to the intestine in bile is sufficient for chylomicron formation and secretion under these conditions.

HFD feeding initially induces rapid weight loss, whereas chronic HFD feeding reduces weight gain in CTα^{IKO} mice

We hypothesized that feeding mice a HFD would increase demand for lipid droplet and chylomicron PC and therefore induce more pronounced changes to the intestinal epithelium of CTα^{IKO} mice. Analysis of three independent

experiments showed that 26% of CTα^{IKO} mice (5 of 19) lost ~25% body weight and displayed steatorrhea between days 4 and 5 following initiation of the HFD, forcing termination of these mice under protocol requirements (**Fig. 2A**). Interestingly, the remaining 74% of CTα^{IKO} mice experienced only modest weight loss, but had significantly less visceral fat mass, lower plasma leptin concentrations, and lower liver TG concentrations than did control mice on day 6 following initiation of the HFD (Fig. 2B–D). Weight loss in CTα^{IKO} mice coincided with reduced food intake (2.76 ± 0.25 g by control mice compared with 1.36 ± 0.21 g by CTα^{IKO} mice between 48 and 72 h after initiation of the HFD; $P = 0.0009$).

The CTα^{IKO} mice fed a HFD for 50 days gained 20% less body weight and had 40% less visceral fat mass compared with controls (Fig. 2E, F). The lower food intake observed in CTα^{IKO} mice compared with control mice in the first week following initiation of the HFD appeared to be an acute response to the diet, as food intake was similar between CTα^{IKO} mice and control mice by week 6 following HFD initiation (2.257 ± 0.16 g/day for control mice compared with 2.034 ± 0.17 g/day for CTα^{IKO} mice; $P = 0.36$). Nevertheless, fasting blood glucose was significantly lower in CTα^{IKO} mice (Fig. 2G). In contrast to liver-specific CTα KO mice (4), fasting plasma TG and cholesterol concentrations

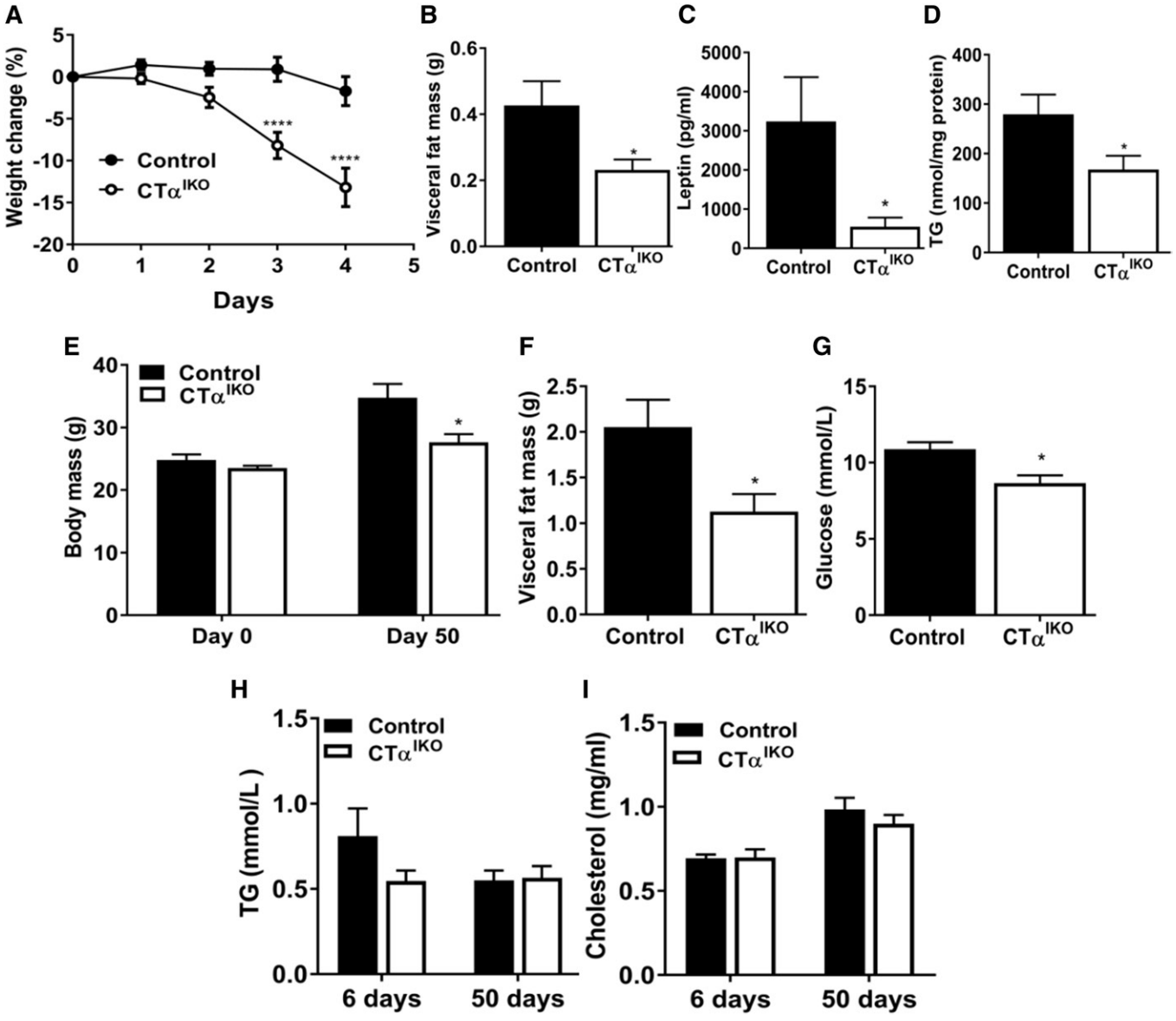

Fig. 2. HFD feeding initially induces rapid weight loss, whereas chronic HFD feeding reduces weight gain, in CTα^{IKO} mice. A: Body mass change relative to total body mass at time of initiation of the HFD; graph is representative of two independent experiments (n = 12 control and 14 CTα^{IKO} mice). Visceral fat mass (B), plasma leptin concentrations (C), and liver TG (D) of control and CTα^{IKO} mice on day 6 following initiation of the HFD (n = 6 per group). E: Body mass of control and CTα^{IKO} mice on days 0 and 50 after initiation of the HFD (n = 5 per group). Visceral fat mass (F) and blood glucose concentrations (G) of control and CTα^{IKO} mice on day 50 after initiation of the HFD (n = 5 per group). Fasting plasma TG (H) and fasting plasma cholesterol (I) concentrations of control mice and CTα^{IKO} mice on days 6 and 50 after initiation of the HFD (n ≥ 5 per group). All mice were female. Values are means ± SEM. * $P < 0.05$; **** $P < 0.0001$.

were not reduced in CTα^{IKO} mice after being fed a HFD for 6 or 50 days (Fig. 2H, I). Taken together, these data show that HFD feeding induces weight loss, whereas chronic feeding reduces weight gain in CTα^{IKO} mice.

Loss of intestinal CTα reduces chylomicron lipidation during HFD feeding

To determine whether impaired dietary lipid absorption contributed to the acute weight loss in CTα^{IKO} mice fed the HFD, we assessed postprandial plasma lipid concentrations. Control and CTα^{IKO} mice were fasted overnight on day 3 following initiation of the HFD (prior to onset of severe weight loss) before refeeding them for 2 h. Food intake was similar between CTα^{IKO} and control mice during HFD refeeding (not shown). Plasma TG concentrations were 60% lower and plasma NEFA concentrations were 30% lower in CTα^{IKO} mice compared with controls after 2 h HFD refeeding (**Fig. 3A**). Furthermore, CTα^{IKO} mice had markedly less TG in the largest lipoprotein fraction compared with controls (Fig. 3B). Interestingly, despite a dramatic difference in plasma TG concentrations between genotypes after refeeding, plasma ApoB concentrations were not different (Fig. 3C). This finding strongly suggests that lipidation of the intestine-derived lipoprotein particles was impaired in CTα^{IKO} mice, whereas the number of particles secreted was not reduced. Total plasma cholesterol concentrations were similar between CTα^{IKO} and control mice after HFD refeeding (Fig. 3A). However, CTα^{IKO} mice had less cholesterol in the largest lipoprotein fraction, whereas HDL cholesterol (Fig. 3D) and plasma ApoA1 concentrations were not different between genotypes (Fig. 3C). To determine whether enhanced particle clearance contributed to the low postprandial plasma TG in CTα^{IKO} mice, we challenged the mice with an intragastric bolus of olive oil after intraperitoneal injection of Poloxamer-407, an inhibitor of lipoprotein lipase. Intestinal TG secretion remained blunted in CTα^{IKO} mice over the 4 h study period (Fig. 3E). Lower plasma TG after refeeding was also observed in CTα^{IKO} mice compared with controls fed a HFD for 6 weeks (1.14 ± 0.06 mmol/l in control mice compared with 0.83 ± 0.09 mmol/l in CTα^{IKO} mice; $P = 0.03$). Taken together, these data show that the intestine secretes TG-poor ApoB-containing particles in the absence of de novo PC synthesis.

Loss of intestinal CTα impairs FA uptake from the intestinal lumen into enterocytes

We hypothesized that impaired intestinal TG secretion in CTα^{IKO} mice was due to TG accumulation in enterocytes. However, CTα^{IKO} mice had significantly lower jejunal TG concentrations than control mice after fasting and refeeding (**Fig. 4A**, B). To track the spatial distribution of FA uptake in the small intestine, we gavaged mice with [^{3}H]-labeled triolein. The radioactivity in the midintestine of CTα^{IKO} mice, where FA absorption is typically highest, was strikingly lower than in control mice (Fig. 4C). As expected based on previous results, the appearance of [^{3}H]-label in plasma was significantly blunted in CTα^{IKO} mice (Fig. 4D). Taken together, these data indicate that loss of intestinal CTα impairs FA uptake from the intestinal lumen into enterocytes in the setting of a HFD.

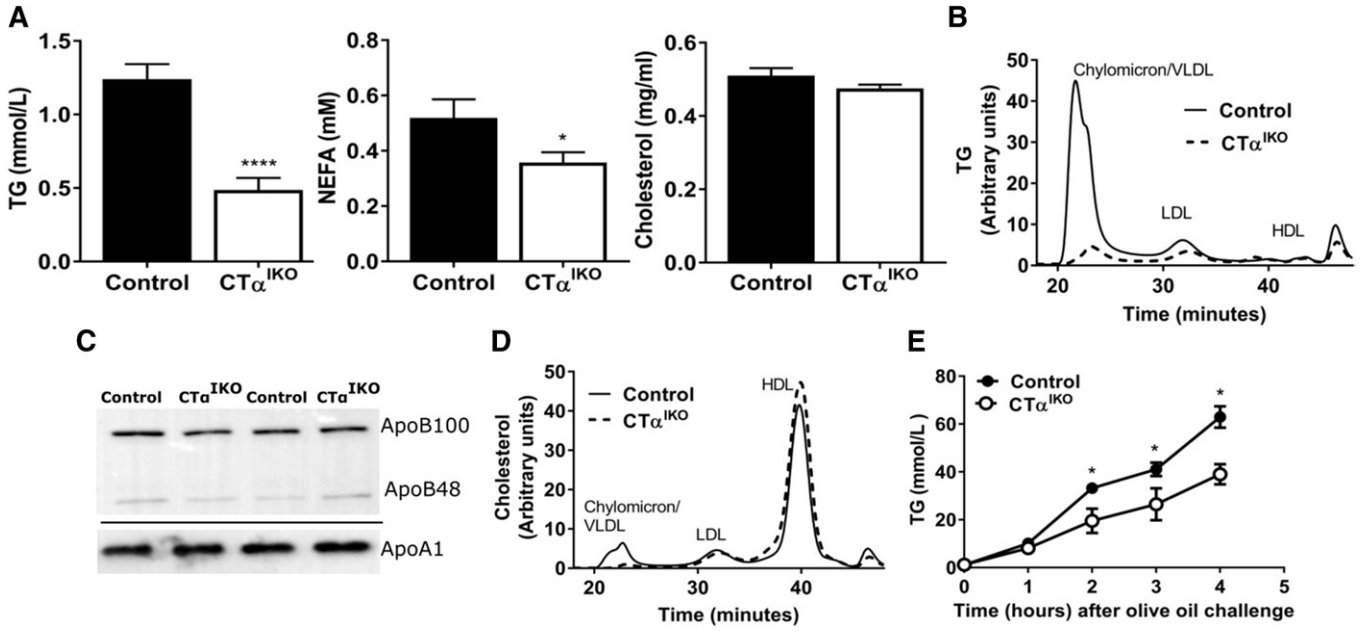

Fig. 3. CTα^{IKO} mice fed a HFD have impaired intestinal TG secretion after a meal. Control and CTα^{IKO} mice were fasted overnight and refed the HFD for 2 h. A: Plasma TG, NEFAs, and cholesterol after refeeding (n = 10 per group). B: FPLC of plasma lipoprotein TG after refeeding (pooled plasma samples from n = 5 per group). C: Representative immunoblot of plasma apolipoproteins after refeeding (ApoB and ApoA1 were run on separate gels). D: FPLC of plasma lipoprotein cholesterol after refeeding (pooled plasma samples from n = 5 per group). E: Plasma TG before and 1, 2, 3, and 4 h following an oral bolus of olive oil and intraperitoneal injection of Poloxamer-407 (n = 4 per group). All mice were female. Values are means ± SEM. * $P < 0.05$; **** $P < 0.0001$.

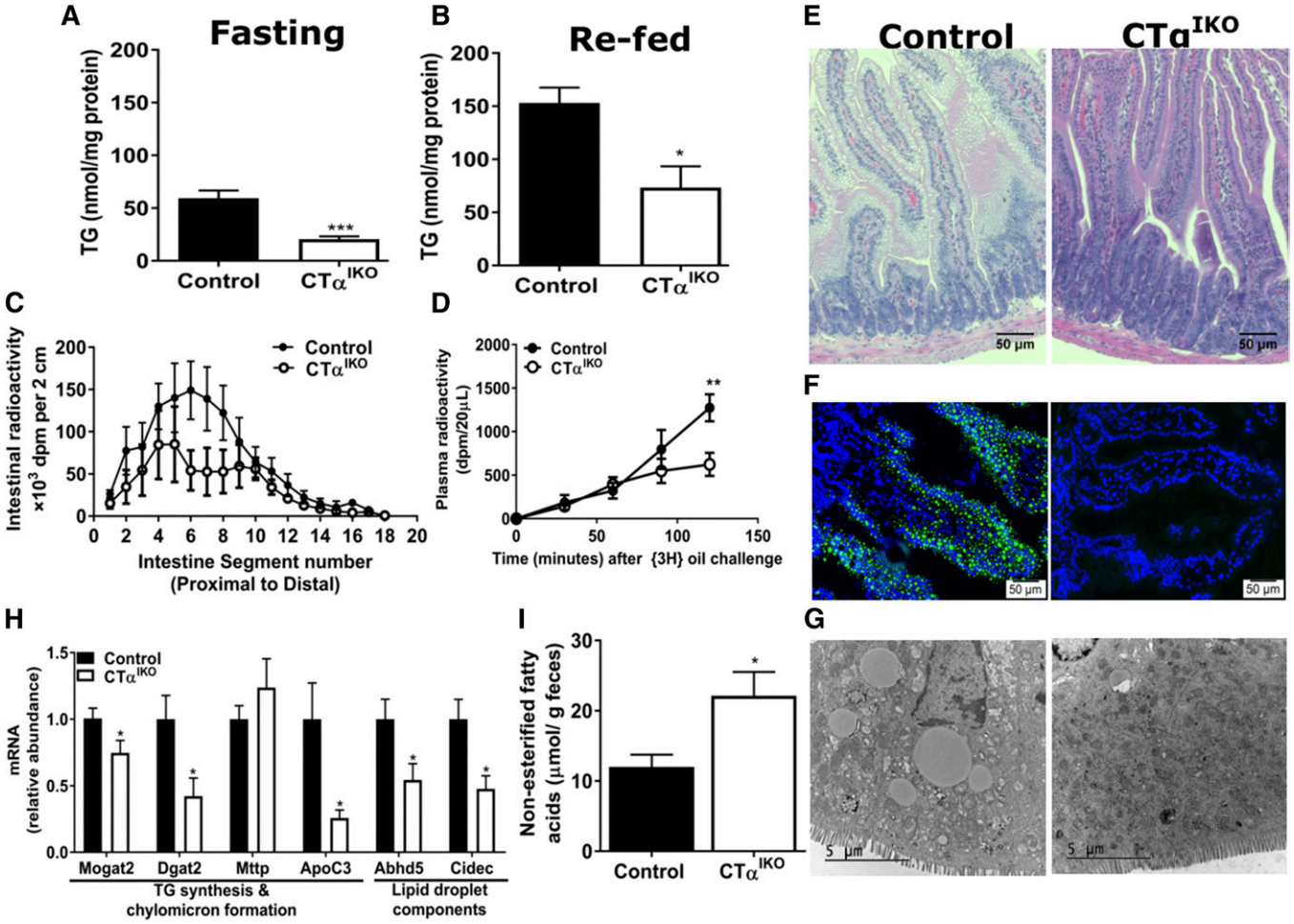

Fig. 4. CTα^{IKO} mice fed a HFD have impaired passage of FAs from the intestinal lumen into enterocytes. Jejunal TG concentrations of female control and CTα^{IKO} mice after fasting (A) or 2 h after refeeding the HFD (B) (n = 5 or 6 per group). Male control and CTα^{IKO} mice were fasted for 4 h on day 3 following initiation of the HFD before receiving an oral bolus of 5 µCi [^{3}H]-labeled triolein in 150 µl of olive oil for 2 h (n = 5 per group). C: Radiolabel in intestine segments 2 h after [^{3}H]-labeled triolein gavage. D: Plasma radiolabel before and 30, 60, 90, and 120 min after a [^{3}H]-labeled triolein gavage. Female control and CTα^{IKO} mice were fasted for 4 h on day 3 following initiation of the HFD before receiving an oral bolus of BODIPY-labeled olive oil. E: Representative H&E-stained proximal intestine sections of control and CTα^{IKO} mice 2 h after oil gavage. F: Fluorescence microscope images of jejunal sections 2 h after BODIPY-labeled oil gavage. G: Representative transmission electron micrographs of jejunal enterocytes 2 h after oil gavage. H: Jejunal mRNA abundance of genes involved in chylomicron and lipid droplet formation (n ⩾ 5 per group). I: FAs in fecal samples from female control and CT α^{IKO} mice (n = 5 per group). Values are means ± SEM. * $P < 0.05$; ** $P < 0.01$; *** $P < 0.001$. Cidec, cell death-inducing DFFA-like effector c; Dgat2, diacylglycerol O-acyltransferase 2; Mttp, microsomal TG transfer protein.

Histological examination of jejunal sections 2 h after a bolus of olive oil revealed fewer lipid droplets in enterocytes of CTα^{IKO} mice compared with control mice fed the HFD (Fig. 4E). We also detected markedly fewer fluorescent lipid droplets in enterocytes of CTα^{IKO} mice gavaged with BODIPY-labeled FAs (Fig. 4F). Moreover, electron microscopy showed a general absence of cytosolic lipid droplets in HFD-fed CTα^{IKO} enterocytes 2 h after an oil challenge (Fig. 4G). Consistent with lower FA concentrations in enterocytes, the mRNA levels of monoacylglycerol O-acyltransferase 2 (*Mogat2*), diacylglycerol O-acyltransferase 2 (*Dgat2*), abhydrolase domain containing 5 (*Abhd5*), and cell death-inducing DFFA-like effector c (*Cidec*) were significantly lower in CTα^{IKO} intestines 2 h after a meal (Fig. 4H). These data suggest that impairment of intestinal PC synthesis reduces FA uptake from the intestinal lumen and thereby limits FA supply for lipid droplet and chylomicron formation. In further support of impaired fat absorption, NEFAs were elevated in feces of CTα^{IKO} mice compared with control mice (Fig. 4I).

Loss of intestinal CTα impairs intestinal cholesterol absorption

Cholesterol concentrations were also significantly higher in feces of CTα^{IKO} mice compared with control mice (**Fig. 5A**). To examine cholesterol turnover, control and CTα^{IKO} mice were administered an oral gavage of [^{3}H]cholesterol and an intravenous injection of [^{14}C]cholesterol, and the labels were measured in plasma and feces over 72 h. After 24 h, the appearance of [^{3}H]cholesterol in the circulation of CTα^{IKO} mice was significantly lower than in control mice (Fig. 5B). Furthermore, cumulative fecal excretion of [^{3}H] neutral sterols over 72 h was higher in CTα^{IKO} mice (Fig. 5C). These data suggest that luminal cholesterol absorption

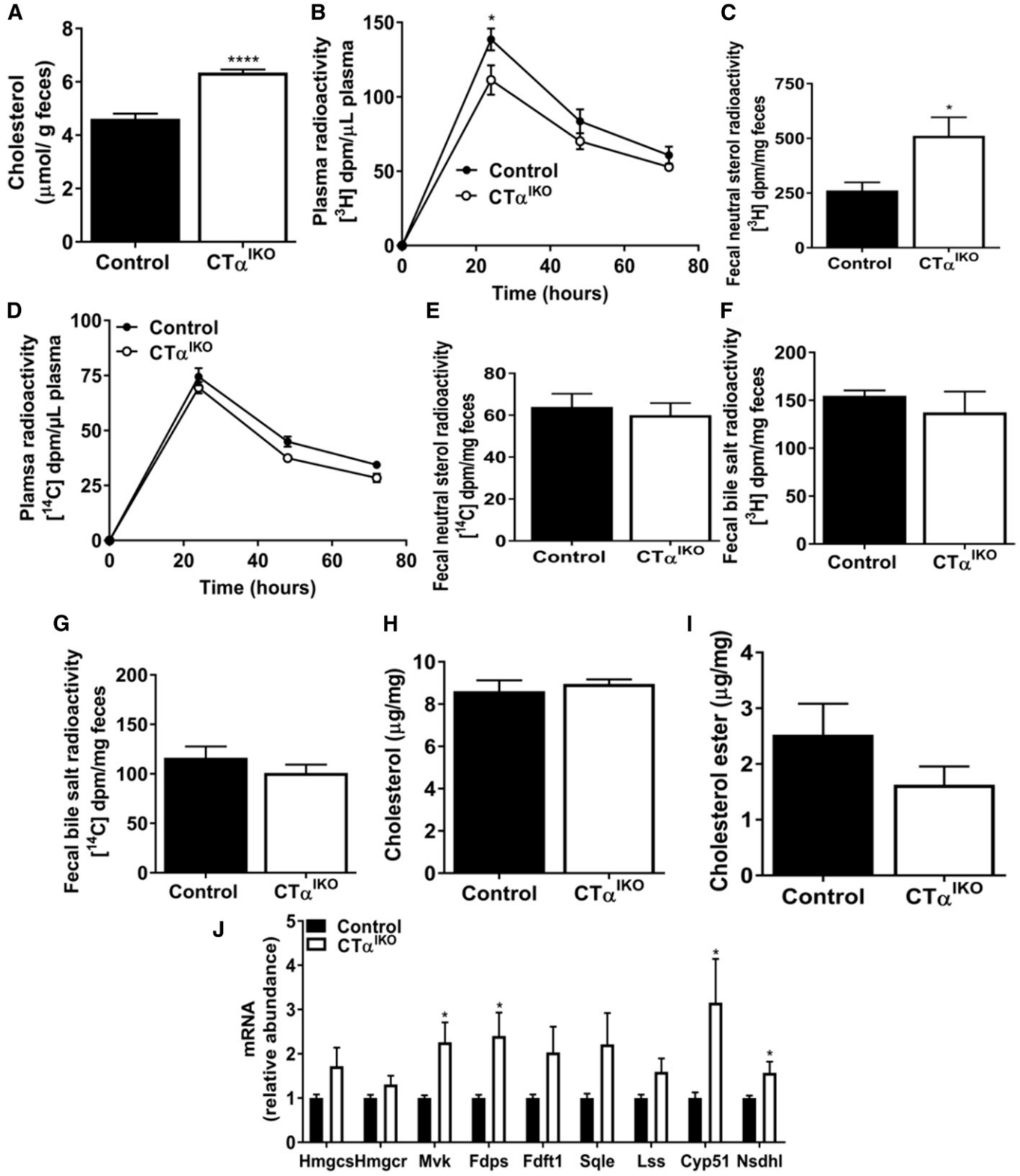

Fig. 5. Loss of intestinal CTα reduces dietary cholesterol absorption. A: Cholesterol in fecal samples from female control and CTα^{IKO} mice (n = 5 per group). Male control and CTα^{IKO} received an oral dose of [^{3}H]cholesterol (2 μCi) with 6 mg of unlabeled cholesterol in 150 μl of olive oil and an intravenous injection of [^{14}C]cholesterol (1 μCi) mixed in Intralipid®. Blood and feces were collected at 24, 48, and 72 h after cholesterol administration (n = 4 per group). B: Plasma [^{3}H]-labeled at 24, 48, and 72 h. C: Cumulative counts in fecal [^{3}H]-labeled neutral sterols over 72 h. D: Plasma [^{14}C]-labeled at 24, 48, and 72 h. E: Cumulative counts in fecal [^{14}C]-labeled neutral sterols over 72 h. Cumulative [^{3}H]-labeled in bile salts (F) and cumulative [^{14}C]-labeled in bile salts (G) over 72 h. Nonesterified cholesterol (H), cholesterol esters (I), and mRNA abundance of cholesterol synthetic genes (J) in the jejunum of control and CTα^{IKO} mice refed the HFD (n = 4 or 5 per group). Values are means ± SEM. * $P < 0.05$; **** $P < 0.0001$. Cyp51, cytochrome P450, family 51; Fdft1, farnesyl-diphosphate farnesyltransferase 1; Fdps, farnesyl diphosphate synthase; Hmgcr, 3-hydroxy-3-methylglutaryl-CoA reductase; Hmgcs, 3-hydroxy-3-methylglutaryl-CoA synthase; Lss, lanosterol synthase; Mvk, mevalonate kinase; Nsdhl, NAD(P)-dependent steroid dehydrogenase-like; Sqle, squalene epoxidase.

is impaired with loss of intestinal CTα. The rate of disappearance of radiolabel from plasma after intravenous injection of [^{14}C]cholesterol and cumulative [^{14}C] accumulation in fecal neutral sterols was not different between genotypes (Fig. 5D, E), suggesting that hepatic cholesterol uptake was unaltered by loss of intestinal CTα. Furthermore, there was no difference in appearance of [^{3}H] or [^{14}C] in fecal bile salts between genotypes, suggesting that hepatic bile acid synthesis was not changed in response to reduced intestinal cholesterol absorption in CTα^{IKO} mice (Fig. 5F, G). Despite impaired cholesterol absorption, jejunal cholesterol and cholesterol ester concentrations were unchanged in CTα^{IKO} mice relative to controls (Fig. 5H, I). Accordingly, mRNA abundance of several genes linked to cholesterol biosynthesis, including mevalonate kinase (*Mvk*), farnesyl diphosphate synthase (*Fdps*), cytochrome P450, family 51 (*Cyp51*), and NAD(P) dependent steroid dehydrogenase-like (*Nsdhl*), were induced in the jejunum of CTα^{IKO} mice relative to controls (Fig. 5J). Induction of intestinal cholesterol biosynthesis in CTα^{IKO} mice might be a compensatory response to impaired cholesterol absorption, or it might be due to altered intestinal phospholipid homeostasis in epithelial cells, as has recently been described (20).

Impaired lipid absorption in CTα^{IKO} mice is linked to reduced expression of plasma membrane lipid transporters

Microvillus length and structure were comparable between genotypes, suggesting that lipid malabsorption in CTα^{IKO} mice is not due to structural damage to the intestinal epithelium (**Fig. 6A**). Intestinal *Lpcat3* deletion in mice reduces passive lipid diffusion into enterocytes by reducing the incorporation of PUFAs into intestinal PC (9, 10). The mRNA levels of *Lpcat3* were not altered in CTα^{IKO} mice relative to controls (Fig. 6B). As expected, jejunal PC concentrations were significantly lower in CTα^{IKO} mice refed the HFD, whereas PE concentrations were unchanged compared with controls (Fig. 6C, D). However, the relative abundance of PC molecular species as measured by mass spectrometry was only minimally different between genotypes, with small increases in the relative abundance of PC (36:2) and PC (38:3) observed in CTα^{IKO} mice (Fig. 6E). To validate our mass spectrometry results, we performed gas-liquid chromatography analysis of the acyl chain constituents of PC and confirmed that the composition of FAs acylated to PC in the proximal intestine was comparable between genotypes (Fig. 6F). Therefore, impaired lipid absorption in CTα^{IKO} mice is not due to changes in the relative abundance of PC molecular species, as observed in mice deficient in intestinal *Lpcat3*. However, an altered PC/PE ratio of intestinal membranes may impair passive lipid diffusion into enterocytes of CTα^{IKO} mice.

The membrane lipid transporters Cluster-determinant 36 (*Cd36*), Solute Carrier Family 27 Member 4 (*Slc27a4;* Fatty acid transport protein 4), and NPC1 like intracellular cholesterol transporter 1 (*Npc1l1*) promote lipid absorption in intestinal epithelial cells (21–23). The mRNA levels of jejunal *Cd36* were dramatically lower in CTα^{IKO} mice relative to control mice (Fig. 6F). Furthermore, *Slc27a4* and *Npc1l1* mRNA levels were modestly lower in CTα^{IKO} mice (Fig. 5F). Therefore, reduced expression of membrane transporters involved in intestinal lipid uptake relative to controls may at least partially account for impaired lipid absorption in CTα^{IKO} mice.

Loss of intestinal CTα enhances postprandial enteroendocrine hormone secretion

Dietary FAs in the lumen of the distal intestine stimulate secretion of enteroendocrine hormones including GLP-1 and PYY from L cells to control food intake and satiety (24). Because CTα^{IKO} mice have impaired FA absorption in the proximal small intestine resulting in increased FA content of feces, we hypothesized that the higher abundance of FAs in the distal small intestine of CTα^{IKO} mice would trigger GLP-1 and PYY secretion. CTα^{IKO} mice had strikingly elevated active GLP-1 (∼9-fold) and PYY (∼9-fold) in plasma 2 h after refeeding the HFD (**Fig. 7A**, B). A major physiological function of GLP-1 is to promote insulin secretion from the pancreas (24). Accordingly, CTα^{IKO} mice had a strong trend toward higher postprandial plasma insulin concentrations compared with controls (Fig. 7C). FGF21 is a hepatokine with multiple systemic effects on carbohydrate and lipid metabolism and is highly responsive to changes in nutrient intake (25–27). Circulating concentrations of FGF21 were 4.5-fold higher in CTα^{IKO} mice compared with controls after HFD refeeding (Fig. 7D). To test whether the observed changes to circulating hormone concentrations altered postprandial glucose metabolism, we refed mice a HFD for 2 h before administering them with an oral glucose challenge. CTα^{IKO} mice had significantly lower peak blood glucose concentrations compared with controls after the glucose challenge (Fig. 7E). Importantly, refed plasma TG and GLP-1 were not different between tamoxifen-treated floxed controls and mice with a heterozygous deletion of intestinal CTα (supplemental Fig. S1N, O). These data link impaired lipid uptake in the absence of intestinal CTα to enhanced postprandial enteric and hepatic hormone secretion, likely contributing to reduced body weight in CTα^{IKO} mice relative to control mice.

Loss of intestinal CTα alters enterohepatic circulation of bile acids and increases biliary PC secretion into the intestinal lumen

We were initially surprised that CTα^{IKO} mice can maintain epithelial cell turnover and intestinal viability in the absence of de novo PC synthesis. Thus, we hypothesized that increased biliary PC secretion may contribute to the maintenance of intestinal PC concentrations and intestinal epithelial cell viability in CTα^{IKO} mice. To examine biliary lipid and bile acid secretion, we cannulated the gallbladders of mice fed the HFD. The rate of bile flow in CTα^{IKO} mice was strikingly higher (∼25%) than in control mice (**Fig. 8A**), coinciding with a doubling of biliary bile acid secretion, a 1.5-fold increase in phospholipid secretion, and a 1.3-fold increase in cholesterol secretion (Fig. 8B–D). Consistent with increased biliary lyso-PC delivery to the intestinal epithelium, the mRNA levels of jejunal lysophosphatidylcholine acyltransferase 4 (*Lpcat4*), which catalyzes

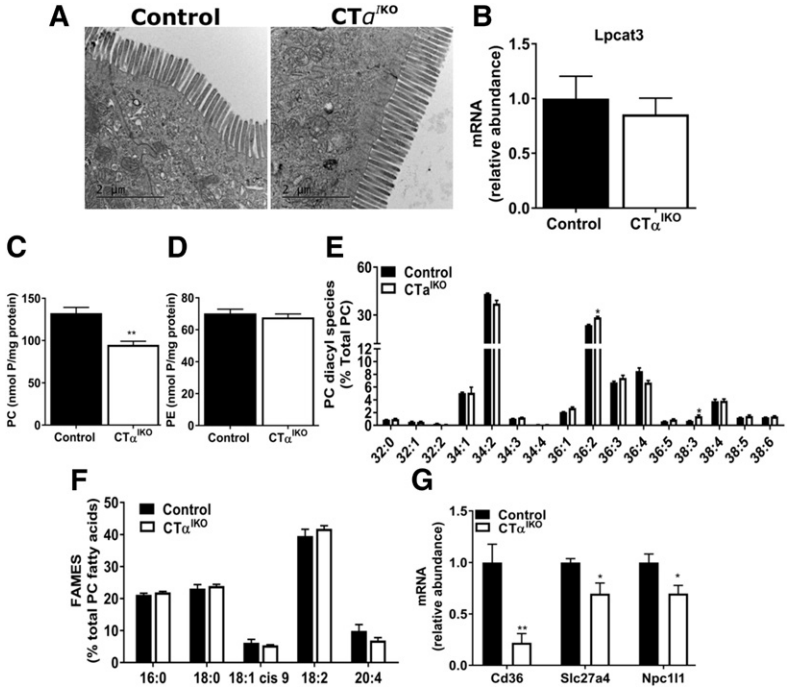

Fig. 6. CTα^{IKO} mice do not have damage to the brush border membrane or changes to relative abundance of jejunal PC molecular species but do have reduced jejunal expression of genes encoding proteins involved in lipid uptake. A: Representative transmission electron micrographs of intestinal microvilli of control and CTα^{IKO} mice fed the HFD. B: *Lpcat3* mRNA abundance in the jejunum of control and CTα^{IKO} mice (n = 5 per group). PC (C) and PE (D) concentrations in the jejunum of control and CTα^{IKO} mice 2 h after HFD refeeding (n = 5 per group). The relative abundance of jejunal PC molecular species (E) and FA methyl esters (FAMES) (F) in PC of control and CTα^{IKO} mice refed the HFD for 2 h (n = 4 or 5 per group). G: mRNA abundance of *Cd36*, *Slc27a4*, and *Npc1l1* in the jejunum of control and CTα^{IKO} mice 2 h after HFD refeeding (n ⩾ 4 per group). All mice were female. Values are means ± SEM. * $P < 0.05$; ** $P < 0.01$.

the addition of oleic acid to lyso-PC (28), was significantly higher in CTα^{IKO} mice 2 h after HFD refeeding (Fig. 8E). Therefore, a higher rate of delivery of biliary PC to the intestines of CTα^{IKO} mice may contribute to their capacity to maintain intestinal epithelial cell viability in the absence of de novo intestinal PC synthesis.

Although total biliary bile acid concentrations were higher in CTα^{IKO} mice, the bile acid species composition was largely unaltered, except for TDCA, which was reduced (Fig. 8F). Consequently, the bile acid hydrophobicity index was similar between control and CTα^{IKO} mice (Fig. 8G). Additionally, a nonsignificant trend toward higher plasma bile acid concentrations in CTα^{IKO} mice fed the HFD was observed (Fig. 8H). There was no change in the hepatic expression of genes involved in bile acid synthesis, and total fecal bile acid concentrations were not different between CTα^{IKO} mice and control mice fed the HFD (Fig. 8I, J). These data strongly indicate that enhanced biliary bile acid and lipid secretion in CTα^{IKO} mice is not driven by an increase in hepatic bile acid synthesis.

There was a robust increase in mRNA levels of the apical sodium-bile acid transporter, *solute carrier family 10 member 2* (*Slc10a2/*ASBT*;* mainly restricted to the ileum under normal conditions), in the jejunum of CTα^{IKO} mice (Fig. 8K). An increase in jejunal ASBT is predicted to increase bile acid absorption in the proximal small intestine and to accelerate enterohepatic cycling of bile acids (29). In line with increased ASBT-mediated bile acid uptake in the proximal small intestine, mRNA levels of the bile-acid transporter Fatty acid binding protein 6 (*Fabp6*) had a strong tendency toward an increase in the jejunum of CTα^{IKO} mice compared with controls 2 h after refeeding. Furthermore, ileal *Slc10a2*, *Fabp6,* and solute carrier family 51 beta subunit (*Slc51b*) mRNA levels were not different, while ileal solute carrier family 51 alpha subunit (*Slc51a*) were lower in CTα^{IKO} mice than in ileums from control mice. Thus, loss of intestinal CTα stimulates the secretion of bile acids and lipids from the liver by a mechanism that involves a shift in reabsorption of bile acids to the proximal small intestine to promote enterohepatic cycling.

DISCUSSION

In this study, we show that intestinal PC synthesis via CTα plays a crucial role in coordinating the metabolic response of mice to HFD feeding. Our data suggest that the

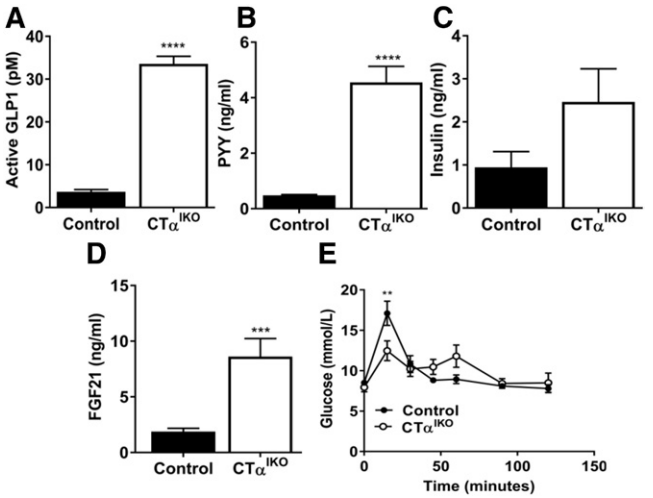

Fig. 7. CTα^{IKO} mice have enhanced GLP-1, PYY, and FGF21 secretion after a high-fat meal. Control and CTα^{IKO} mice were fasted overnight on day 3 following initiation of the HFD before being refed for 2 h. A: Plasma active GLP-1 (n = 5 per group). B: Plasma PYY (n = 10 per group). C: Plasma insulin (n = 10 per group). D: Plasma FGF21 (n = 10 per group). E: Blood glucose concentrations in control and CTα^{IKO} mice refed the HFD for 2 h followed by an oral bolus of glucose. All mice were female. Values are means ± SEM. ** $P < 0.01$; *** $P < 0.001$; **** $P < 0.0001$.

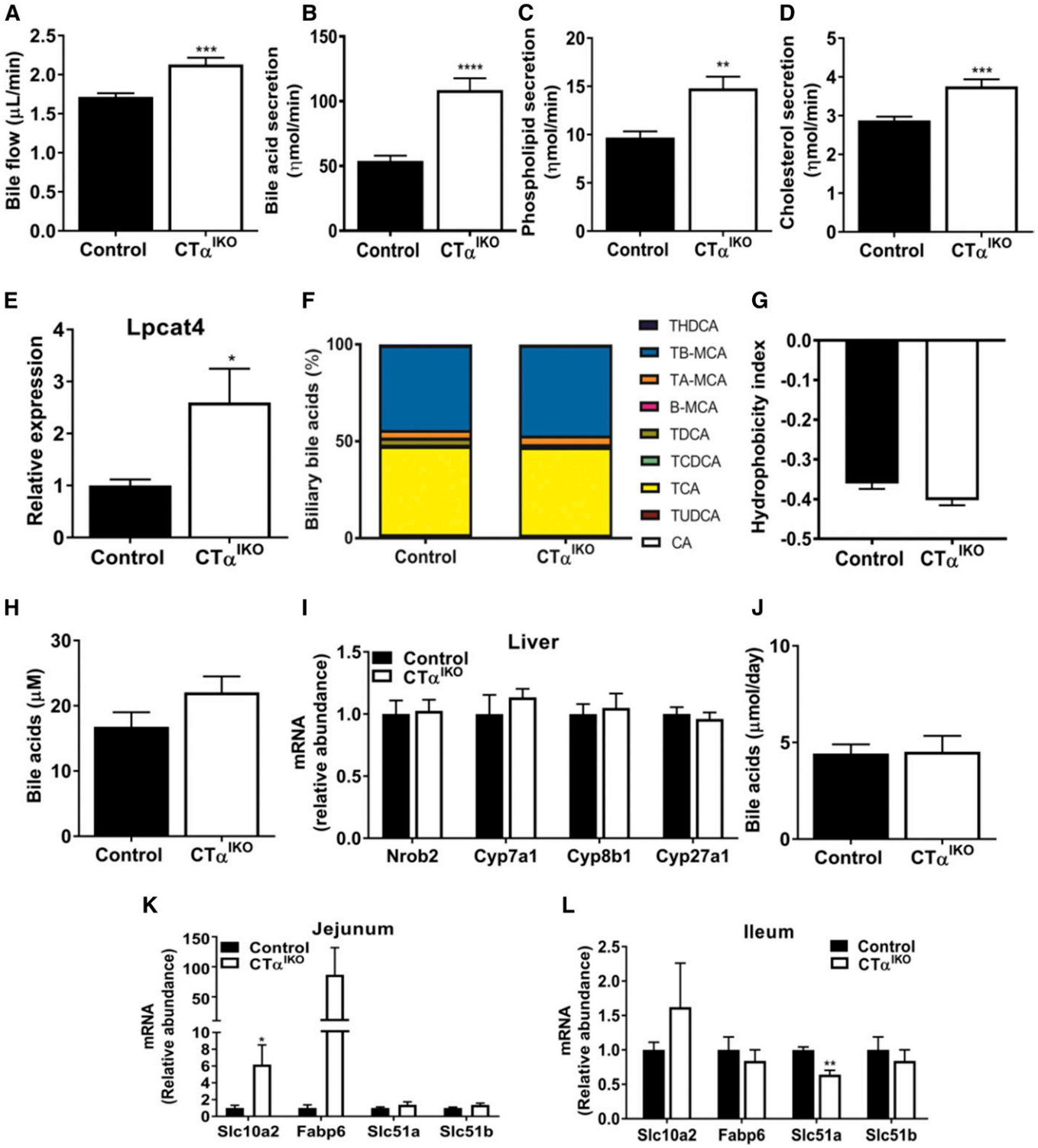

Fig. 8. Loss of intestinal CTα enhances biliary bile acid secretion. Gallbladders of male control and CTα^{IKO} mice were cannulated, and bile was collected in preweighed containers (n = 6–8 per group). A: Bile flow. B: Bile salt secretion. C: Phospholipid secretion. D: Cholesterol secretion. E: Jejunal *Lpcat4* expression. F: Relative biliary bile acid composition. G: Bile acid hydrophobicity index. H: Plasma bile acids. I: mRNA abundance of hepatic genes involved in bile acid synthesis. J: Fecal bile acids. mRNA abundance of jejunal bile-acid responsive genes (K) (n ⩾ 4 per group) and mRNA abundance of ileal bile acid-responsive genes in control and CTα^{IKO} mice 2 h after refeeding the HFD (L) (n = 3 per group). Values are means ± SEM. * $P < 0.05$; ** $P < 0.01$; *** $P < 0.001$; **** $P < 0.0001$. B-MCA, β-β-muricholic acid; CA, cholic acid; Cyp7a1, cytochrome P450, family 7 subfamily a member 1; Cyp8b1, cytochrome P450, family 8 subfamily b member 1; Cyp27a1, cytochrome P450, family 27 subfamily a member 1; Fabp6, FA binding protein 6; Nrob2, nuclear receptor subfamily 0 group b member 2; TA-MCA, tauro-α-muricholic acid; TB-MCA, tauro-β-muricholic acid; TCA, taurocholic acid; TCDCA, taurochenodeoxycholic acid; THDCA, taurohyodeoxycholic acid; TUDCA, tauroursodeoxycholic acid.

metabolic response to a HFD in CTα^{IKO} mice is driven by a combination of impaired dietary lipid absorption, increased secretion of the fat-induced satiety hormones GLP-1 and PYY, and reduced food intake. Furthermore, a shift in expression of bile acid-responsive genes to the proximal small intestine of CTα^{IKO} mice is linked to accelerated enterohepatic bile acid cycling. Loss of intestinal CTα is not well tolerated by some mice fed a HFD, indicating that de novo PC synthesis is specifically required for normal intestinal metabolic function. Furthermore, our data show that reacylation of lyso-PC from the intestinal lumen cannot compensate for loss of CTα-derived PC in enterocytes.

Mice with intestinal deletion of the gene encoding the PC remodeling enzyme LPCAT3 have reduced chylomicron secretion when fed a chow diet due to failure to incorporate PUFAs into intestinal PC, which alters membrane dynamics and FA uptake (9, 10). In contrast, we found that de novo PC synthesis is not required for chylomicron secretion in the setting of a low-fat diet. This observation suggests that the reacylation of lyso-PC derived from bile can fully accommodate chylomicron assembly under these conditions. However, an increase in cellular FA concentrations increases cellular demand for PC to maintain membrane lipid homeostasis and produce the surface monolayer for lipid droplets and lipoproteins (2). Accordingly, HFD-fed CTα^{IKO} mice have disrupted intestinal metabolic function (likely due to constant influx of FAs into intestinal epithelial cells, which increases cellular PC demands), including impaired dietary lipid uptake (despite minimal changes to the relative abundance of polyunsaturated PC species or *Lpcat3* expression in the intestine). Therefore, both pathways for intestinal PC formation (i.e., de novo PC synthesis and PC remodeling) are independently required for dietary lipid absorption when consuming a HFD. Furthermore, LPCAT3-deficient mice do not experience changes in bile acid concentrations (10), suggesting that the pathways of de novo PC synthesis and PC remodeling also control distinct aspects of enterohepatic physiology.

We used a radiolabeled tracer to demonstrate that CTα^{IKO} mice fed a HFD have impaired jejunal FA uptake, resulting in the production of chylomicrons with lower TG content. Impaired lipid uptake in mice lacking intestinal de novo PC synthesis is not due to gross damage to the intestinal epithelium, as electron microscopy revealed an intact brush border membrane. Instead, loss of intestinal CTα is linked to intestinal metabolic dysfunction in the setting of a HFD, including reduced expression of genes involved in dietary lipid absorption. Targeted deletion of *Mogat2* (13), *Cd36* (21), *Abhd5* (30), and *Npc1l1* (23), all of which are lower in the intestines of CTα^{IKO} mice relative to controls, impairs dietary lipid absorption. Therefore, intestinal de novo PC synthesis apparently maintains a network of genes involved in dietary lipid uptake.

The intestinal epithelium is highly active in cell division, growth, differentiation, and secretion; that is, processes that require adequate PC supply (2). Therefore, we were surprised that CTα^{IKO} mice can maintain epithelial cell turnover and intestinal viability in the absence of de novo intestinal PC synthesis. Nevertheless, increased biliary PC secretion may contribute to the maintenance of intestinal PC concentrations in CTα^{IKO} mice. We unexpectedly found that deletion of intestinal CTα doubles the rate of biliary bile acid secretion in CTα^{IKO} mice compared with control mice. Because bile acids drive bile flow as well as biliary cholesterol and phospholipid secretion, these parameters were also significantly higher in CTα^{IKO} mice (31). The higher rate of delivery of bile acids (with similar composition to bile acids in controls) into the intestinal lumen of CTα^{IKO} mice implies that impaired FA absorption with loss of intestinal CTα is not due to a deficiency of mixed micelles required for efficient fat absorption. Furthermore, because the cholesterol-labeling study, the analysis of fecal bile output, and measurement of the expression of bile acid-synthetic genes revealed that hepatic bile acid synthesis is not induced by loss of intestinal CTα, enterohepatic cycling of bile acids is likely accelerated. This hypothesis is supported by a shift in expression of *Slc10a2* and *Fabp6* toward more proximal parts of the small intestine. A shift in the expression of bile acid-responsive genes to the proximal intestine has been reported previously in mice lacking intestinal GATA4, a transcription factor that controls jejunal–ileal identity (32, 33). The change in spatial expression of bile acid-responsive genes in intestinal GATA4-deficient mice is also linked to impaired lipid absorption (33) and increased bile flow (29). Clearly, the molecular mechanisms that regulate cross-talk between the intestine and liver in controlling bile formation in CTα^{IKO} mice require further research. Changes to enterohepatic circulation of bile acids can influence lipid, carbohydrate, and energy metabolism (34). Furthermore, bile acids increase the circulating level of FGF21 (35), a hepatokine that is increased in CTα^{IKO} mice and that reduces adiposity when administered pharmacologically (25). Therefore, changes in bile acid metabolism may contribute to metabolic adaptations in the CTα^{IKO} mice fed a HFD.

GLP-1 and PYY are hormones that can influence energy balance through both the enteric nervous system and peripheral targets after nutrient-induced secretion from L cells (24). Under normal conditions, most dietary FAs are absorbed in the proximal small intestine (Fig. 4C). However, if high concentrations of FAs reach L cells of the distal intestine, they can enhance GLP-1 and PYY secretion (24). Accordingly, mice with intestinal deletion of genes involved in dietary fat absorption, including *Mogat2* (13), diacylglycerol O-acyltransferase 1 (*Dgat1*) (36), and *Lpcat3* (10), have relatively high postprandial plasma GLP-1 concentrations. Similarly, impaired HFD absorption in the proximal small intestine of CTα^{IKO} mice allows FAs to reach the distal intestine to potentiate enteroendocrine hormone secretion. The stimulation of GLP-1 and PYY secretion by FAs in CTα^{IKO} mice likely contributes to their relatively more severe response to a HFD compared with a chow diet, as was observed in intestine-specific LPCAT3-deficient mice (10). High postprandial plasma GLP-1 is associated with increased insulin secretion and lower blood glucose concentrations in CTα^{IKO} mice compared with control mice fed a HFD. Furthermore, enhanced GLP-1-mediated insulin

secretion might account for the lower plasma-free FA concentrations in CTα^{IKO} mice compared with controls by suppressing lipolysis in adipocytes. Additionally, enhanced PYY secretion in CTα^{IKO} mice could contribute to their reduced body weight by interacting with brain regions that control energy balance (37). Taken together, our findings demonstrate that modulation of intestinal phospholipid metabolism can influence whole-body physiology by enhancing the secretion of metabolically active hormones.

In conclusion, this study demonstrates that intestinal de novo PC synthesis plays a central role in dietary lipid absorption during HFD feeding. Loss of intestinal CTα amplifies postprandial GLP-1 and PYY secretion and alters circulating glucose and FFA concentrations, linking gut phospholipid synthesis to whole-body nutrient disposal and metabolism. Our studies also reveal an unexpected role for intestinal de novo PC synthesis in the maintenance of normal enterohepatic circulation of bile acids, potentially by governing the spatial expression of the bile-acid transporter *Slc10a2* in the intestine. Therefore, a physiologically normal response to dietary fat intake depends on de novo PC synthesis in the intestinal epithelium, and the reacylation of PC derived from extraintestinal sources cannot fulfill this requirement.

The authors thank Dr. Patricia Brubacker for Villin-CreER^{T2} mice; Nicole Coursen, Susanne Lingrell, Ying Wayne Wang, Rongjia Liu, and Dr. Kunimasa Suzuki for technical assistance; Audric Moses and the University of Alberta Lipidomics Core Facility; Drs. Jean Vance, Dennis Vance, and Richard Lehner for critical evaluation of the manuscript; Ms. Ruth Jacobs for critical editing of the grant; Priscilla Guo and Dr. Xuejun Sun for assistance with electron microscopy; Amy Barr of the University of Alberta Cardiovascular Research Centre; and Lynette Elder of the Alberta Diabetes Institute Histology Core.

REFERENCES

1. van der Veen, J. N., J. P. Kennelly, S. Wan, J. E. Vance, D. E. Vance, and R. L. Jacobs. 2017. The critical role of phosphatidylcholine and phosphatidylethanolamine metabolism in health and disease. *Biochim. Biophys. Acta.* **1859:** 1558–1572.
2. Cornell, R. B., and N. D. Ridgway. 2015. CTP:phosphocholine cytidylyltransferase: Function, regulation, and structure of an amphitropic enzyme required for membrane biogenesis. *Prog. Lipid Res.* **59:** 147–171.
3. Wang, L., S. Magdaleno, I. Tabas, and S. Jackowski. 2005. Early embryonic lethality in mice with targeted deletion of the CTP:phosphocholine cytidylyltransferase alpha gene (Pcyt1a). *Mol. Cell. Biol.* **25:** 3357–3363.
4. Jacobs, R. L., C. Devlin, I. Tabas, and D. E. Vance. 2004. Targeted deletion of hepatic CTP:phosphocholine cytidylyltransferase alpha in mice decreases plasma high density and very low density lipoproteins. *J. Biol. Chem.* **279:** 47402–47410.
5. Noga, A. A., Y. Zhao, and D. E. Vance. 2002. An unexpected requirement for phosphatidylethanolamine N-methyltransferase in the secretion of very low density lipoproteins. *J. Biol. Chem.* **277:** 42358–42365.
6. Nilsson, A. 1968. Intestinal absorption of lecithin and lysolecithin by lymph fistula rats. *Biochim. Biophys. Acta.* **152:** 379–390.
7. Parthasarathy, S., P. V. Subbaiah, and J. Ganguly. 1974. The mechanism of intestinal absorption of phosphatidylcholine in rats. *Biochem. J.* **140:** 503–508.
8. Voshol, P. J., D. M. Minich, R. Havinga, R. P. Elferink, H. J. Verkade, A. K. Groen, and F. Kuipers. 2000. Postprandial chylomicron formation and fat absorption in multidrug resistance gene 2 P-glycoprotein-deficient mice. *Gastroenterology.* **118:** 173–182.
9. Li, Z., H. Jiang, T. Ding, C. Lou, H. H. Bui, M. S. Kuo, and X. C. Jiang. 2015. Deficiency in lysophosphatidylcholine acyltransferase 3 reduces plasma levels of lipids by reducing lipid absorption in mice. *Gastroenterology.* **149:** 1519–1529.
10. Wang, B., X. Rong, M. A. Duerr, D. J. Hermanson, P. N. Hedde, J. S. Wong, T. Q. Vallim, B. F. Cravatt, E. Gratton, D. A. Ford, et al. 2016. Intestinal phospholipid remodeling is required for dietary-lipid uptake and survival on a high-fat diet. *Cell Metab.* **23:** 492–504.
11. Tso, P., H. Kendrick, J. A. Balint, and W. J. Simmonds. 1981. Role of biliary phosphatidylcholine in the absorption and transport of dietary triolein in the rat. *Gastroenterology.* **80:** 60–65.
12. el Marjou, F., K. P. Janssen, B. H. Chang, M. Li, V. Hindie, L. Chan, D. Louvard, P. Chambon, D. Metzger, and S. Robine. 2004. Tissue-specific and inducible Cre-mediated recombination in the gut epithelium. *Genesis.* **39:** 186–193.
13. Yen, C. L., M. L. Cheong, C. Grueter, P. Zhou, J. Moriwaki, J. S. Wong, B. Hubbard, S. Marmor, and R. V. Farese. 2009. Deficiency of the intestinal enzyme acyl CoA:monoacylglycerol acyltransferase-2 protects mice from metabolic disorders induced by high-fat feeding. *Nat. Med.* **15:** 442–446.
14. Folch, J., M. Lees, and G. H. Sloane Stanley. 1957. A simple method for the isolation and purification of total lipides from animal tissues. *J. Biol. Chem.* **226:** 497–509.
15. Alnouti, Y., I. L. Csanaky, and C. D. Klaassen. 2008. Quantitative-profiling of bile acids and their conjugates in mouse liver, bile, plasma, and urine using LC-MS/MS. *J. Chromatogr. B Analyt. Technol. Biomed. Life Sci.* **873:** 209–217.
16. Heuman, D. M. 1989. Quantitative estimation of the hydrophilic-hydrophobic balance of mixed bile salt solutions. *J. Lipid Res.* **30:** 719–730.
17. Zhou, X., and G. Arthur. 1992. Improved procedures for the determination of lipid phosphorus by malachite green. *J. Lipid Res.* **33:** 1233–1236.
18. Mashige, F., K. Imai, and T. Osuga. 1976. A simple and sensitive assay of total serum bile acids. *Clin. Chim. Acta.* **70:** 79–86.
19. Myher, J. J., and A. Kuksis. 1984. Determination of plasma total lipid profiles by capillary gas-liquid chromatography. *J. Biochem. Biophys. Methods.* **10:** 13–23.
20. Wang, B., X. Rong, E. N. D. Palladino, J. Wang, A. M. Fogelman, M. G. Martín, W. A. Alrefai, D. A. Ford, and P. Tontonoz. 2018. Phospholipid remodeling and cholesterol availability regulate intestinal stemness and tumorigenesis. *Cell Stem Cell.* **22:** 206–220.e4.
21. Drover, V. A., M. Ajmal, F. Nassir, N. O. Davidson, A. M. Nauli, D. Sahoo, P. Tso, and N. A. Abumrad. 2005. CD36 deficiency impairs intestinal lipid secretion and clearance of chylomicrons from the blood. *J. Clin. Invest.* **115:** 1290–1297.
22. Stahl, A., D. J. Hirsch, R. E. Gimeno, S. Punreddy, P. Ge, N. Watson, S. Patel, M. Kotler, A. Raimondi, L. A. Tartaglia, et al. 1999. Identification of the major intestinal fatty acid transport protein. *Mol. Cell.* **4:** 299–308.
23. Altmann, S. W., H. R. Davis, L. J. Zhu, X. Yao, L. M. Hoos, G. Tetzloff, S. P. Iyer, M. Maguire, A. Golovko, M. Zeng, et al. 2004. Niemann-Pick C1 Like 1 protein is critical for intestinal cholesterol absorption. *Science.* **303:** 1201–1204.
24. Cummings, D. E., and J. Overduin. 2007. Gastrointestinal regulation of food intake. *J. Clin. Invest.* **117:** 13–23.
25. Fisher, F. M., and E. Maratos-Flier. 2016. Understanding the physiology of FGF21. *Annu. Rev. Physiol.* **78:** 223–241.
26. Badman, M. K., P. Pissios, A. R. Kennedy, G. Koukos, J. S. Flier, and E. Maratos-Flier. 2007. Hepatic fibroblast growth factor 21 is regulated by PPARalpha and is a key mediator of hepatic lipid metabolism in ketotic states. *Cell Metab.* **5:** 426–437.
27. Kharitonenkov, A., T. L. Shiyanova, A. Koester, A. M. Ford, R. Micanovic, E. J. Galbreath, G. E. Sandusky, L. J. Hammond, J. S. Moyers, R. A. Owens, et al. 2005. FGF-21 as a novel metabolic regulator. *J. Clin. Invest.* **115:** 1627–1635.
28. Hishikawa, D., H. Shindou, S. Kobayashi, H. Nakanishi, R. Taguchi, and T. Shimizu. 2008. Discovery of a lysophospholipid acyltransferase family essential for membrane asymmetry and diversity. *Proc. Natl. Acad. Sci. USA.* **105:** 2830–2835.
29. Out, C., J. V. Patankar, M. Doktorova, M. Boesjes, T. Bos, S. de Boer, R. Havinga, H. Wolters, R. Boverhof, T. H. van Dijk, et al. 2015. Gut microbiota inhibit Asbt-dependent intestinal bile acid reabsorption via Gata4. *J. Hepatol.* **63:** 697–704.

30. Xie, P., F. Guo, Y. Ma, H. Zhu, F. Wang, B. Xue, H. Shi, J. Yang, and L. Yu. 2014. Intestinal Cgi-58 deficiency reduces postprandial lipid absorption. *PLoS One.* **9:** e91652.
31. Verkade, H. J., R. J. Vonk, and F. Kuipers. 1995. New insights into the mechanism of bile acid-induced biliary lipid secretion. *Hepatology.* **21:** 1174–1189.
32. Bosse, T., C. M. Piaseckyj, E. Burghard, J. J. Fialkovich, S. Rajagopal, W. T. Pu, and S. D. Krasinski. 2006. Gata4 is essential for the maintenance of jejunal-ileal identities in the adult mouse small intestine. *Mol. Cell. Biol.* **26:** 9060–9070.
33. Battle, M. A., B. J. Bondow, M. A. Iverson, S. J. Adams, R. J. Jandacek, P. Tso, and S. A. Duncan. 2008. GATA4 is essential for jejunal function in mice. *Gastroenterology* **135**: 1676–1686.e1.
34. Cariou, B., K. van Harmelen, D. Duran-Sandoval, T. H. van Dijk, A. Grefhorst, M. Abdelkarim, S. Caron, G. Torpier, J. C. Fruchart, F. J. Gonzalez, et al. 2006. The farnesoid X receptor modulates adiposity and peripheral insulin sensitivity in mice. *J. Biol. Chem.* **281:** 11039–11049.
35. Cyphert, H. A., X. Ge, A. B. Kohan, L. M. Salati, Y. Zhang, and F. B. Hillgartner. 2012. Activation of the farnesoid X receptor induces hepatic expression and secretion of fibroblast growth factor 21. *J. Biol. Chem.* **287:** 25123–25138.
36. Ables, G. P., K. J. Yang, S. Vogel, A. Hernandez-Ono, S. Yu, J. J. Yuen, S. Birtles, L. K. Buckett, A. V. Turnbull, I. J. Goldberg, et al. 2012. Intestinal DGAT1 deficiency reduces postprandial triglyceride and retinyl ester excursions by inhibiting chylomicron secretion and delaying gastric emptying. *J. Lipid Res.* **53:** 2364–2379.
37. Stadlbauer, U., M. Arnold, E. Weber, and W. Langhans. 2013. Possible mechanisms of circulating PYY-induced satiation in male rats. *Endocrinology.* **154:** 193–204.